• Basic Research •

Laser photocoagulation improves the transduction efficiency of lentivirus vectors injected intravitreally

Jian Jiao[1], Yi-Jun Xu[1], Xue-Dong Li[2], Wen Hua[2], Yan-Rong Jiang[3]

[1]Department of Ophthalmology, People's Hospital of Beijing Daxing District, Beijing 102600, China
[2]Department of Ophthalmology, Beijing Chaoyang Hospital, Capital Medical University, Beijing 100020, China
[3]Department of Ophthalmology, People's Hospital, Peking University People's Hospital, Beijing 100044, China
Correspondence to: Jian Jiao. Department of Ophthalmology, People's Hospital of Beijing Daxing District, Beijing 102600, China. drjiaojian@163.com
Received: 2025-03-15 Accepted: 2026-02-25

Abstract

• **AIM:** To evaluate the effect of laser photocoagulation on transfection efficiency of lentivirus (LV) vectors injected intravitreally.

• **METHODS:** The rat retina was photocoagulated prior to intravitreal injection of LV vectors encoding red fluorescent protein. Rats given intravitreal injection or photocoagulation alone served as controls. The transduction efficiency was analyzed by fundus angiography, histopathology, and immunofluorescence staining. Potential adverse effect of laser photocoagulation was evaluated in choroid flat mounts by observing the morphology of retinal pigment epithelium (RPE) that formed the outer blood-retina barrier.

• **RESULTS:** Laser photocoagulation enhanced the retinal area transduced by LV vectors in fundus images and increased the maximum transduction thickness in histopathological sections. Choroid flat mounts showed the RPE transduced by LV vectors maintained normal morphology.

• **CONCLUSION:** Laser photocoagulation improves the transduction efficiency of LV vectors injected intravitreally, identifying this as a promising gene therapy strategy for inherited retinal dystrophies caused by gene mutations in RPE and photoreceptor cells.

• **KEYWORDS:** gene therapy; laser photocoagulation; lentivirus vector; transduction efficiency; intravitreal injection
DOI:10.18240/ijo.2026.06.05

Citation: Jiao J, Xu YJ, Li XD, Hua W, Jiang YR. Laser photocoagulation improves the transduction efficiency of lentivirus vectors injected intravitreally. *Int J Ophthalmol* 2026;19(6):1057-1064

INTRODUCTION

The favorable anatomical, accessibility, and immunological characteristics of the retina make it an optimal target tissue for gene therapy[1]. In the last decades, some remarkable achievements have been made in gene therapy of inherited retinal dystrophies (IRDs)[2]. Approval of Luxturna (voretigene neparvovec-rzyl), the first gene therapy product for Leber congenital amaurosis 2, by the U.S. Food and Drug Administration marked a new era of retinal gene therapy[3].

Gene therapy usually requires the use of vectors, such as adeno-associated viruses (AAVs) and lentivirus (LV), to introduce the target gene into the host cell. Currently, AAVs are considered the most promising viral vectors in the field of gene therapy because they possess several favorable features, such as nonpathogenicity, minimal immunogenicity, the ability to transduce nondividing cells, and the capacity to mediate sustained expression of the therapeutic gene[4-5]. For this reason, more than one hundred AAV serotypes have been isolated according to the sequence of their capsid protein[3]. However, despite the popularity of AAVs, they are difficult to use in transduction of the outer retina by intravitreal injection because of the presence of physical barriers[6-7]. In addition, the packaging capacity of AAVs is less than 5 kb[7]. These obstacles preclude the use of AAVs in therapy for some IRDs, such as Stargardt maculopathy, when the disease is caused by mutations of large genes with coding sequences that exceed 5 kb[8]. Therefore, considerable effort has been made to explore alternative vectors that have larger packaging capacities. LV vectors possess transgene cargo capacity of approximately 8–10 kb, and are considered an attractive alternative to the primate lentiviral vectors for gene therapy[9].

Vectors administration methods for IRDs gene therapies usually involve subretinal or intravitreal injection[2,4]. Intravitreally administered virus vectors can transduce the inner retina with high efficiency[10]; however, the majority of genes mutated in IRDs are expressed in retinal pigment epithelium (RPE) and photoreceptor (PR) of the outer retina[11]. By contrast, subretinal injection can transduce the RPE and PR directly, as it releases the viral vectors into the subretinal space[12]. For example, Luxturna is delivered subretinally by an AAV2 vector to treat RPE65-related Leber congenital amaurosis 2[13].

However, both subretinal and intravitreal injection present some limitations. Subretinal injection is an invasive technique that requires delicate surgical operations and complex procedures with high iatrogenic risk[14]. Intravitreal injection is less invasive, but it is hindered by physical barriers, such as the internal limiting membrane (ILM) that is particularly thick in adult and large animals[6]. These barriers decrease the ability of intravitreally injected viral vectors to effectively transduce the RPE and PR in outer retina[15]. The diffusion of viral vectors from the vitreous to the outer retina can increase if the ILM is peeled surgically or if the physical retinal barrier is digested with a nonspecific protease or disrupted by advanced retinal degeneration[6,15].

Studies have suggested that LV vectors are usually inefficient at transducing the outer retinal cells following intravitreal injection because of their larger size and the physical barriers of retina[16]. The surgical challenges and high iatrogenic risks of subretinal injection led us to suppose that vitreous injection would be a more practical approach for administration of gene therapy if some simple and less invasive methods could promote penetration of the viral vectors through the retinal barriers. In our preliminary experiments, we found that laser photocoagulation destroyed the retinal barriers and seemed to increase the transduction efficiency of intravitreally injected LV vectors. The aim of the present study was to verify this possibility using LV vectors encoding red fluorescent protein (RFP). LV vectors normally possess a large packaging capacity but transduce the RPE and PR with low efficiency. The vectors were injected intravitreally immediately after laser photocoagulation, and the transduction efficiency was analyzed by Micron III fundus angiography, histopathology, and immunofluorescence staining. Choroid flat mounts were examined to detect potential adverse effects.

MATERIALS AND METHODS

Ethical Approval Animals were handled following the Guide of the ARVO Statement for the Use of Animals in Ophthalmic and Vision Research, and this study was approved by People's Hospital of Beijing Daxing District Ethics Committee (approval number: BLARC-LAWER-202509007).

LV Vectors Construction and Titration LV vectors encoding the RFP and a multiple repetitive nonsense sequence (5'-TTCTCCGAACGTGTCACGT-3') were constructed by Genechem Co., Ltd., Shanghai, China. Briefly, 293 T cells were transduced with the following plasmids: pGCSIL-RFP carrier, pHelper 1.0 carrier, and pHelper 2.0 carrier. Plasmids were digested by restriction endonuclease Age I/EcoRI, and oligonucleotides were annealed and ligated with linearized PGCSIL-RFP by T4 DNA ligase. The recombinants were finally identified by enzyme cutting and sequencing. The LV vectors were produced in 293 T packaging cells, and the concentrations were titered to 9×10^8 TU/mL. The RFP-LV vectors were used to transduce intestinal epithelial cell line (IEC)-6 cells to test the transduction efficiency.

Animals Normal adult male Brown Norway rats were procured (weight ranged from 250 to 300 g) from Vital River Laboratories (Beijing, China). A total of 30 Brown Norway rats were divided into 3 equal groups. Before the experiments, every eye was examined using direct ophthalmoscopy to exclude abnormalities.

Laser Photocoagulation and Intravitreal Injection The right eyes of the first group of rats were given laser photocoagulation, and the left eyes did not receive any treatments as the normal control. The right eyes of the second group rats were injected intravitreally with LV vectors but not given the laser photocoagulation. The right eyes of the third group rats were photocoagulated and then injected intravitreally with LV vectors immediately after laser photocoagulation.

For the laser photocoagulation, the pupils were dilated with tropicamide (5 mg/mL) and phenylephrine hydrochloride (5 mg/mL), and the rats were anesthetized with an intraperitoneal injection of pentobarbital (30 mg/kg). A total of 8 spots were photocoagulated between the retinal vessels in a peripapillary distribution at a distance of approximately 2-3 disc diameters with the following laser parameters: 100 mW, 100 μm, 521 nm, and 50ms (Coherent Novus 2000, USA). The right eyes from the second and third groups of rats were injected intravitreally with 5 μL LV vectors using a 30-gauge micro-injector (Hamilton Co., USA) under a microscope. A coverslip filled with 0.5% methylcellulose was used as a contact lens for direct viewing of the fundus during these procedures.

Fundus Fluorescein Angiography The area transduced by LV vectors was determined by fundus fluorescein angiography (FFA) carried out 7d after intravitreal injection. After mydriasis and anesthesia, the rats were intraperitoneally injected with 10% fluorescein sodium (0.1 mL/kg), and the early-phase angiograms were obtained with a Micron III instrument (Phoenix Laboratories, USA) within 1-3min after fluorescein sodium injection.

Histopathology and Immunofluorescence Staining Five rats from every group were euthanatized at 7d after intravitreal injection. The right eyes from the three groups of rats were enucleated, embedded in optimum cutting temperature compound (TissueTek, Sakura Finetek Inc., Japan), and directly frozen in a cryostat (Leica CM1900, Germany) at -20°C. Serial 6 μm frozen sections were cut along the vertical meridian, and sections crossing the laser lesion were selected. The left eyes of the first group rats were also used to produce frozen sections and served as the normal control. These frozen sections were blocked for 2h in phosphate buffered saline

containing 5% bovine serum albumin and 1% Triton X-100, and stained with 4',6-diamidino-2-phenylindole (Invitrogen, USA) to label the nuclei. The sections were viewed with a fluorescence microscope (Eclipse 50i, Nikon, Japan) and photographed.

Choroid Flat Mounts At 7d after intravitreal injection, five rats from every group were euthanatized for choroid flat mounts by the method described previously[17]. Briefly, the rats were anesthetized and perfused through the left ventricle with 1 mL phosphate buffered saline containing 50 mg/mL fluorescein isothiocyanate-dextran (2×10^6 average molecular weight; Sigma, USA). All the right eyes from the three groups and the left eyes form the first group were enucleated and fixed in 4% paraformaldehyde for 1h at room temperature. The anterior segment and sensory retina were carefully removed. Four to six radial relaxing incisions were made from the edge to the equator to allow the RPE-choroid-sclera complex to be flattened onto a glass slide with the RPE facing up. The flat mounts were photographed with laser confocal microscopy (LSM700; Carl Zeiss, Germany).

Statistical Analysis ImageJ software (National Institutes of Health, USA) was used to quantify the data from the fundus angiograms and histopathological sections. The angiograms captured by the Micron III were used to calculate the area ratio of the transduced retina with red fluorescence to total retina with background green fluorescence. The maximum thickness of RFP expression in the frozen sections was also measured. All values are presented as mean±standard error of the mean (SEM) and compared by Tukey's repeated-measures one-way analysis of variance with SPSS V20.0 (SPSS Inc., USA). $P<0.05$ was considered statistically significant.

RESULTS

Laser Photocoagulation Increased the Area of the Retina Transduced by LV Vectors The Micron III fundus camera is designed to capture high-resolution FFA images of rodent animals. The Micron III allowed direct *in vivo* observation of the red fluorescence from retinas transduced by the RFP-LV vectors. The FFA images of normal eyes (laser-/Lv- group) showed bright green fluorescence of fluorescein sodium in the vessels and dim green background fluorescence, but no red fluorescence (Figure 1A). The eyes treated with laser photocoagulation only (laser+/Lv- group) showed normal green fluorescence and leakage of fluorescein sodium at the laser lesions, but again no red fluorescence (Figure 1B). The eyes injected intravitreally with LV vectors but without laser photocoagulation (laser-/Lv+ group) showed no obvious red fluorescence at the posterior retina around the optic papilla. Three of ten eyes in the laser-/Lv+ group showed red RFP fluorescence in the peripheral retina at the puncture point of the intravitreal injection (Figure 1C, white arrow). Eyes given both the laser photocoagulation and intravitreal injection (laser+/Lv+ group) showed substantial red fluorescence at the posterior retina around the optic papilla, and leakage of fluorescein sodium was observed only at the laser lesions (Figure 1D). The red fluorescence could be observed more clearly with the red channel of the Micron III (Figure 1E). Calculation and comparison of the area ratios of the transduced retina with red fluorescence to the total fundus revealed statistically significant differences between the laser+/Lv+ group and the other three groups (Figure 1F).

Laser Photocoagulation Significantly Enhanced the Maximum Transduction Thickness of Histopathological Sections Frozen sections showed disorganization of the retina at the laser lesions and revealed the distribution pattern of red fluorescence at the transduced retina. The tissue structure of the normal retina in the laser-/Lv- group is shown in Figure 2A, and no red fluorescence was evident at any layer of retina. In the laser+/Lv- group, the normal structure of retina was disrupted at the laser lesions, but no red fluorescence was detected either (Figure 2B). In the laser-/Lv+ group, intravitreal injection just resulted in very slight red fluorescence at the level of RPE, but retina retained its normal structure (Figure 2C). The higher magnification made the frozen sections more sensitive to detect RFP than the fundus images, so slight expression of RFP could be observed in the frozen sections (Figure 2C), but no obvious red fluorescence was detected at the posterior retina around the optic papilla in the fundus images by Micron III (Figure 1C). By contrast, the laser+/Lv+ group showed both disorganization of the retina at the laser lesions and extensive red fluorescence around the laser lesions (Figure 2D). In the horizontal direction, the red fluorescence extended from the laser lesions to the periphery and formed the "expansion regions" of transduction around the laser lesion. Hence, if two laser lesions were located adjacent to each other, the "expansion regions" of transduction showed contact and mutual integration (Figure 2E), which corresponded to the substantial red fluorescence observed around the optic papilla in the Micron III fundus images (Figure 1D). Moreover, the retina at the "expansion regions" of transduction still remained normal morphology (Figure 2E). In the vertical direction, laser photocoagulation significantly enhanced the transduction thickness. The maximum range of RFP distributed from the outer plexiform layer to the choroid, including the RPE and PR. Measurement of the maximum thickness of RFP expression in frozen sections with ImageJ software revealed statistically significant differences among the groups (Figure 2F).

Choroid Flat Mounts Showed the RPEs Transduced by LV Vector Maintained Normal Morphology The hexagonal RPEs in choroid flat mounts could be observed by laser confocal microscopy when they expressed RFP. Because

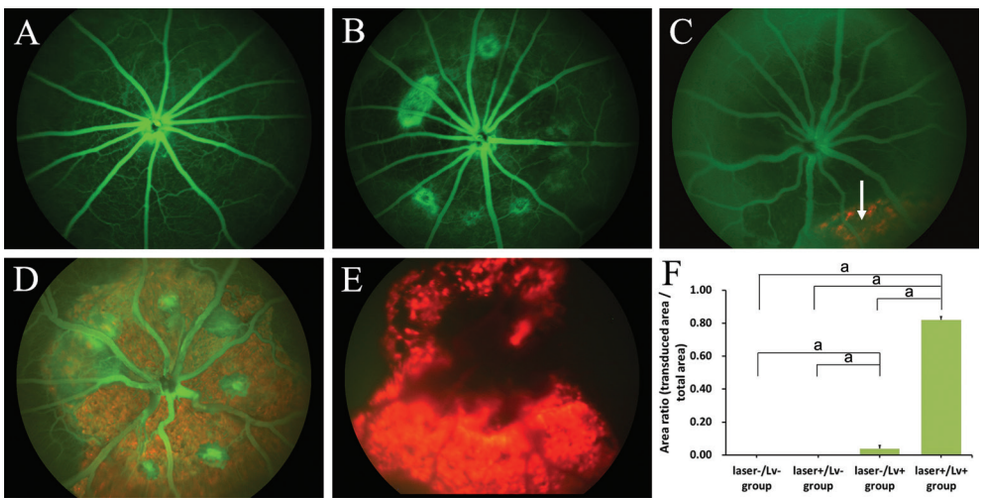

Figure 1 Laser photocoagulation increased the area of the retina transduced by LV vectors A: Fundus angiography of the laser-/Lv- group showed bright green fluorescence of fluorescein sodium in the vessel and dim green background fluorescence, but no red fluorescence; B: Fundus angiography of the laser+/Lv- group showed normal green fluorescence and leakage of fluorescein sodium at the laser lesions, but no red fluorescence of red fluorescent protein (RFP); C: Fundus angiography of the laser-/Lv+ group did not show obvious red fluorescence at the posterior retina around the optic papilla, but the peripheral retinas at three of ten eyes showed red fluorescence apparently adhering to the puncture point of the intravitreal injection (white arrow); D: Fundus angiography of the laser+/Lv+ group showed substantial red fluorescence at the posterior retina around the optic papilla and fluorescein sodium leakage at the laser lesions; E: The red fluorescence could be observed more clearly with the red channel of the Micron III; F: Mean values for the area ratio of transduced retina to total fundus are shown as mean±SEM, and analyzed with Tukey's repeated-measures one-way analysis of variance. [a]P<0.01. Lv: Lentivirus; SEM: Standard error of the mean.

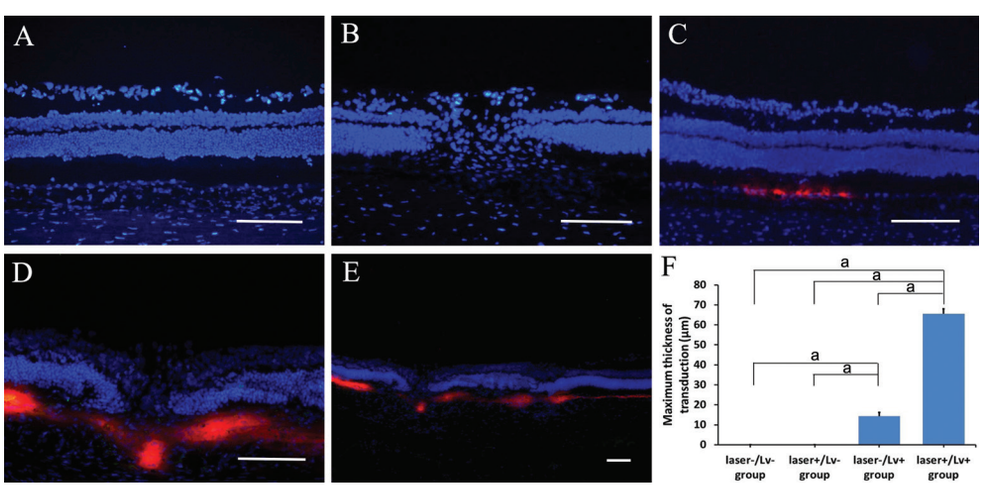

Figure 2 Laser photocoagulation significantly enhanced the maximum transduction thickness of histopathological sections A: Frozen sections of the laser-/Lv- group showed a normal retinal structure; B: The laser+/Lv- group showed disorganization of the retina at the laser lesions but no red fluorescence; C: The intravitreal injection at the laser-/Lv+ group only resulted in slight red fluorescence in the RPE which retained its normal structure; D: The laser+/Lv+ group showed both disorganization of retina at the laser lesions and extensive red fluorescence around laser lesions. The maximum range of RFP extended from the outer nuclear layer to the choroid, including the RPE and PR; E: The transduction "expansion region" was significantly greater than the laser lesion. Two laser lesions distributed relatively adjacent to each other showed contact and mutual integration of the transduction "expansion regions"; F: Mean values for the maximum thickness of the RFP are shown as mean±SEM, and were analyzed with Tukey's repeated-measures one-way analysis of variance. [a]P<0.01. Scale bar: 100 μm. RPE: Retinal pigment epithelium; RFP: Red fluorescent protein; PR: Photoreceptor; SEM: Standard error of the mean; Lv: Lentivirus.

no RPE expressed RFP, flat mounts from laser-/Lv- group and laser+/Lv- group showed only the green fluorescence of the fluorescein isothiocyanate–dextran perfused into the choroid capillary (Figure 3A-3B). In the laser-/Lv+ group, only sporadic RPEs expressing RFP were observed in flat mounts around the optic papilla (Figure 3C, white arrow), which corresponded well with the finding of only a few RPEs transduced by LV in Figure 2C. By contrast, the flat mounts of the laser+/Lv+ group showed extensive hexagonal RPEs that expressed RFP and maintained normal morphology at the

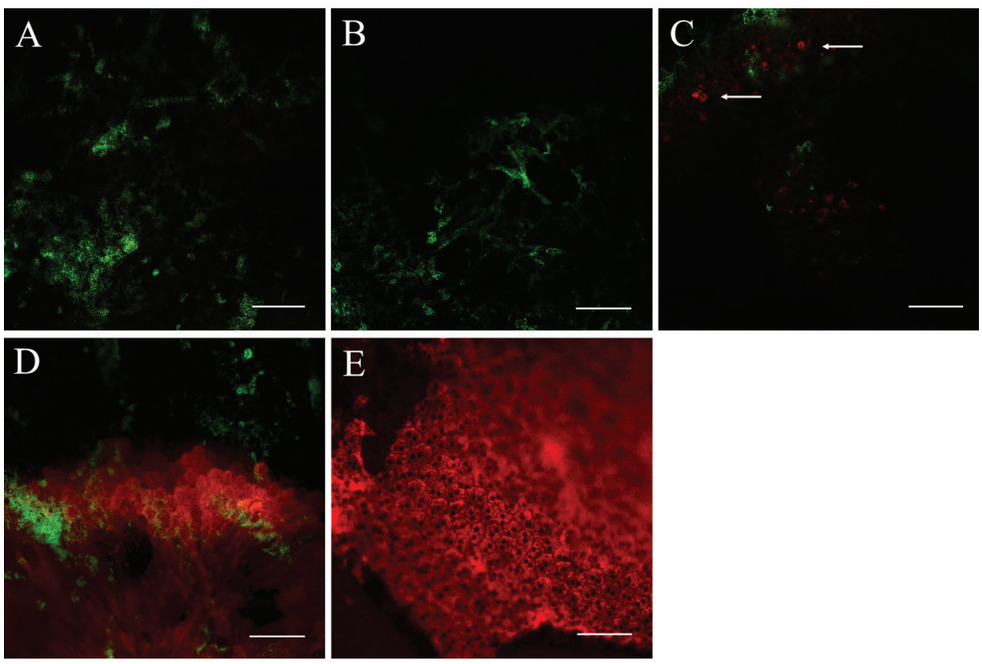

Figure 3 Choroid flat mounts confirmed a normal morphology for the transduced RPE in the expansion region A-B: Flat mounts of the laser-/Lv- and laser+/Lv- groups showed only the green fluorescence of fluorescein isothiocyanate–dextranperfused into the choroid capillary; C: The flat mounts of the laser-/Lv+ group showed sporadic RPEs expressing RFP around the optic papilla (white arrow); D: The flat mounts of the laser+/Lv+ group showed extensive RPEs expression the RFP at the posterior retina around the optic papilla; E: The red channel of the laser confocal microscope showed that the transduced RPEs with two nuclei at transduction expansion regions retained their normal hexagonal shape and tight arrangement, indicating that the outer blood-retina barrier was maintained in its normal state. Scale bar: 100 μm. RPE: Retinal pigment epithelium; RFP: Red fluorescent protein; Lv: Lentivirus.

posterior retina around the optic papilla (Figure 3D). These tightly arranged hexagonal RPEs located in the transduction "expansion regions" were observed more clearly in the red channel of laser confocal microscope (Figure 3E).

DISCUSSION

Gene mutations expressed in the RPE and PR account for the majority of IRDs, and about half of all known IRDs are caused by mutations in genes whose coding sequence exceeds 5 kb[18]. The packaging capacity of AAVs was less than 5 kb, and subretinal injection was the preferred route of delivery because AAVs reach cells in outer retina difficultly when intravitreally administered. Many investigators have explored alternative vectors, such as the LV that has a transgene cargo capacity of approximately 8-10 kb and can efficiently integrate its genome into a host cell for stable gene expression. Furthermore, LV vectors are not pathogenic after gene delivery and their increased safety features can facilitate their clinical application[3].

Subretinal injections are more technically challenging and invasive, as they require creation of a hole in the retina by the vitrectomy surgeon and detachment of the PR from the RPE with the injection of fluid. This surgical procedure is therefore accompanied by a higher risk of iatrogenic complications, such as foveal thinning, macular holes, choroidal effusion, retinal detachment, and hemorrhage[10,19-20]. Intravitreal injection is relatively safe; however, it does not effectively transduce cells in the outer retina because of the presence of physical barrier. The vitreous and ILM form the physical barrier to transduction and result in the failure of vectors delivered intravitreally to transduce RPE and PR in outer retina[21]. For this reason, we investigated laser photocoagulation as a method to overcome the physical barriers, and we expected to enhance the transduction efficiency of intravitreally injected LV vectors with larger packaging capacity.

In this study, we used the Micron III fundus camera to watch the retina transduced and determine the transduced area. This instrument was specifically developed to produce high-resolution fundus images in rodents. In a previous report, the Micron III was used in quantitative research of choroidal neovascularization in rats[22]. To our knowledge, this study was the first use of the Micron III to quantify the ratio of the transduced area in an experimental study of gene therapy. The Micron III revealed the red fluorescence of retinas transduced by RFP-LV vectors *in vivo* and reduced the numbers of rodent animals sacrificed for invasive methods.

Of course, the Micron III still has a lower magnification capability than light microscopes, so the fundus images obtained with the Micron III were less sensitive than the frozen sections for detecting the red fluorescence (Figure 1C *vs* Figure 2C). In the laser-/Lv+ group, the fundus images were

not sufficiently sensitive to detect the slight red fluorescence from the RPE transduced by LV vectors at the posterior retina around the optic papilla, although red fluorescence was observed in the peripheral retina, adhering to the puncture point of intravitreal injection, in three of 10 eyes (Figure 1C, white arrow). Conversely, frozen sections were sensitive enough to reveal slight expression of RFP from the RPE transduced by LV vectors at the posterior retina around the optic papilla (Figure 2C). We speculate that the peripheral transduced retina originated from the destruction of the retinal barrier by the intravitreal injection puncture, but this speculation could not be verified directly in the present study. For this reason, we did not exclude the area of the peripheral transduced retina when we calculated the area ratio. The presence of the peripheral transduced retina would increase the area ratio of the transduced retina to the total retina in the fundus images; but even so, this average area ratio was still significantly lower for the laser-/Lv+ group than for the laser+/Lv+ group (Figure 1F).

RPE cells carry out many important functions, such as absorption of scattered light, the conversion and storage of retinoid, fluid transport, and the phagocytosis and autophagy functions[23]. In addition, normal RPE cells show a hexagonal appearance and are arranged tightly *via* tight junction complexes to form the outer blood-retina barrier[24]. Disorders of the RPE cells can result in a series of ocular fundus diseases[25]. The flat mounts of the laser+/Lv+ group (Figure 3E) showed substantial numbers of transduced hexagonal RPE cells at the transduction expansion regions and they were tightly arranged in the normal morphology, as reported previously[26]. Correspondingly, the fundus images obtained with the Micron III showed that the leakage of fluorescein sodium in the laser+/Lv+ group occurred only at the locations of laser lesions, but no leakage occurred at the extensive transduction expansion regions (Figure 1D). Taken together, these results indicated that the outer blood-retina barrier composed of RPE transduced by RFP-LV vectors was maintained in its normal state except for the positions of laser lesions.

Subretinal delivery remains the most efficient administration route for gene therapy when targeting the RPE and PR. However, the disadvantages mentioned above cannot be ignored and have led to many attempts to enhance the transduction efficiency of intravitreal injection. For example, Dalkara *et al*[27] reported that digesting the ILM with nonspecific protease improved the efficiency of AAV-mediated transduction in nonhuman primates. Similarly, Takahashi *et al*[6] achieved efficient transduction through surgical ILM peeling. Lee *et al*[28-29] were the first to demonstrate laser photocoagulation enhancement of AAV vector transduction of the mouse retina. We confirmed that laser photocoagulation significantly improved the transduction efficiency of LV vectors injected intravitreally. In addition, LV mainly infected the outer retina, including the RPE and PR.

Among the three methods used to improve transduction efficiency, laser photocoagulation is the most conventional and well-established therapy, and it has been widely applied for various retinal diseases because of easy operation with little iatrogenic risk. Previous research indicated that laser photocoagulation resulted in a stable scar after 2mo[30]. The diameter, distribution density, and burn intensity of laser lesions could be well controlled according to the specific clinical requirements[28]. The retinal morphology at the transduction expansion regions also remained roughly normal (Figure 2E). Taken together, these findings indicated that laser photocoagulation had very little impact on the whole retina, just with damage limited to the laser lesions. Compared with subretinal injections, the combination of laser photocoagulation and intravitreal injection of LV vectors seemed to be an efficient and safe method for transduction of the outer retina, as it was less invasive and seldom induced retinal detachment and other iatrogenic complications.

The mechanism of outer retina transduction by intravitreally injected LV vectors after laser photocoagulation is not completely clear. Thermal disruption of the retina barrier certainly played an important role in this process[28], as previous studies had indicated that various retinal barrier disruptions, such as surgical ILM peeling or digestion of ILM with nonspecific protease treatment[6,27], could enhance retinal transduction. Mechanisms other than simple thermal disruption were likely also involved in the robust transduction. For example, laser-stimulated Müller cell activation and the movement of Müller cell endfeet might disrupt the ILM[31]. Nonetheless, we think these viewpoints seem suitable to explain the enhanced transduction in the vertical direction at the laser lesions. In the horizontal direction, the significant transduction expansion regions around the laser lesions indicated that additional mechanisms perhaps accounted for the enhanced transduction by laser photocoagulation. We hypothesized an alteration of cytokine secretion such as matrix metalloproteinase 9 (MMP-9), or activation of macrophages around the laser lesions, as reported in previous studies[32-33], might have participated in the enhanced transduction. In further research, to confirm the safety of laser photocoagulation, we plan to validate the impact of disrupting the inner limiting membrane of retinal through visual electrophysiology, and explore the maximum safe photocoagulation dose that the retina can tolerate. Comprehensive understanding of the findings in this study provided an assumption that the transduction procedure enhanced by laser photocoagulation occurred as shown in the schematic diagram in Figure 4. The

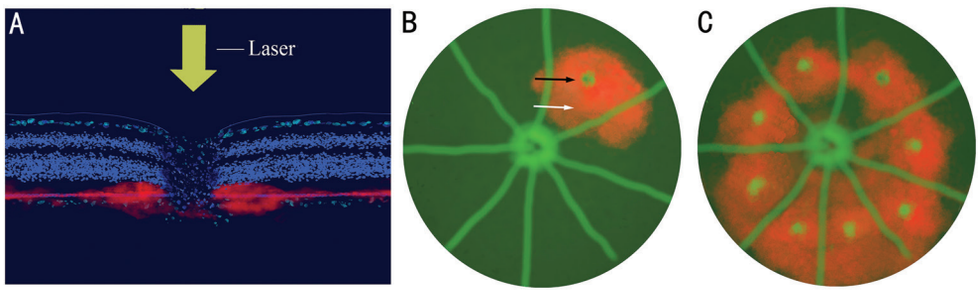

Figure 4 Schematic diagram of the retina transduction enhanced by laser photocoagulation A: The retinal physical barrier was destroyed at laser lesion by the thermal disruption of photocoagulation and other possible mechanisms, which led to extensive retinal transduction. The transduced region spread around and beyond the range of the laser lesion; B: The laser lesion (black arrow) actually acted as the "anchor point" for the transduction process, and the transduced retina around the "anchor point" formed the "expansion region" (white arrow); C: Reasonable arrangement of the laser lesions allowed the transduction expansion regions to come into contact and integrate mutually, resulting in a widespread transduction area at the posterior retina.

physical barriers were destroyed at the laser lesions and LV vectors penetrated the sensory retina from the vitreous to the RPE (Figure 4A); therefore, the laser lesions actually acted as an "anchor point" for the transduction procedure. Once the retina was penetrated by the LV vectors at the "anchor points", the transduction would continue to spread. In the vertical direction, the transduced depth was distributed from the outer nuclear layer to the choroid, including the RPE and PR (Figure 4A). In the horizontal direction, the transduced area around the laser lesions spread and formed the expansion region (Figure 4B). Interestingly, the diameter of the transduction expansion region was significantly greater than that of the laser lesions. The diameter ratio of the expansion region to the laser lesion generally averaged about fivefold, with a maximum of tenfold. The existence of an expansion region was very important for improving the transduction efficiency. Researchers could reasonably arrange the distribution density of laser lesions so that expansion regions of two laser lesions would contact each other and integrate mutually. These reasonably arranged laser lesions would generate a widespread transduction area with fewer laser lesions (Figure 4C). Obviously, fewer laser lesions would reduce the damage to the retinal function, which was the most favored goal in gene therapy of IRDs. According to this method, fewer but reasonably well-arranged laser lesions would also allow researchers to transduce a specific region of retina, such as the macula of humans and other primates, which was not suitable for direct photocoagulation. Certainly, the barriers against transduction, such as the ILM in large animals, were particularly thick[6,34]. Whether laser photocoagulation could overcome this barrier to enhance transduction efficiency in large animals remained to be confirmed in the future.

In summary, we demonstrated that laser photocoagulation significantly improved the transduction efficiency of LV vectors injected intravitreally. We also observed that the retina retained a normal structure in the expansion region and the outer blood-retina barrier formed by transduced RPE remained intact and arranged tightly in its normal morphology. These findings indicated that the combination of laser photocoagulation and intravitreal injection of LV vectors seemed to be an efficient and safe method for gene therapy. This method enabled LV vectors with large cargo capacity to transduce the outer retina with low iatrogenic risk. Therefore, photocoagulation provides a new strategy for gene therapy of various IRDs caused by large gene mutations in the RPE and PR, such as Stargardt maculopathy and Usher syndrome.

ACKNOWLEDGEMENTS

Authors' Contributions: Jiao J performed most of the experiments, wrote the manuscript, contributed to the study concept and design, and are responsible for the integrity of the work as a whole; Xu YJ performed animal experiments, interpreted data, and wrote the manuscript; Li XD performed animal experiments; Hua W supervised the project, and interpreted data; Jiang YR designed the experiments, supervised the project. All authors read and approved the manuscript.

Foundation: Supported by the Joint Laboratory Special Project Foundation of People's Hospital of Beijing Daxing District (No.4202440531).

Conflicts of Interest: Jiao J, None; **Xu YJ,** None; **Li XD,** None; **Hua W,** None; **Jiang YR,** None.

REFERENCES

1 Ebner LJA, Grimm C. AAV serotypes and their suitability for retinal gene therapy. *Adv Exp Med Biol* 2023;1415:131-134.

2 Butt FR, Dhivagaran T, Li B, *et al*. Gene therapy for inherited retinal disease: current strategies, personalized medicine, and future implications—a comprehensive review. *J Pers Med* 2025;15(12):619.

3 Ziccardi L, Cordeddu V, Gaddini L, *et al*. Gene therapy in retinal dystrophies. *Int J Mol Sci* 2019;20(22):5722.

4 Lee SH, Kong YJ, Lyu J, *et al*. Laser photocoagulation induces transduction of retinal pigment epithelial cells by intravitreally

administered adeno-associated viral vectors. *Hum Gene Ther Meth* 2015;26(5):159-161.

5 Fu Q, Polanco A, Lee YS, *et al*. Critical challenges and advances in recombinant adeno-associated virus (rAAV) biomanufacturing. *Biotech & Bioengineering* 2023;120(9):2601-2621.

6 Takahashi K, Igarashi T, Miyake K, *et al*. Improved intravitreal AAV-mediated inner retinal gene transduction after surgical internal limiting membrane peeling in cynomolgus monkeys. *Mol Ther* 2017;25(1): 296-302.

7 Marrone L, Marchi PM, Azzouz M. Circumventing the packaging limit of AAV-mediated gene replacement therapy for neurological disorders. *Expert Opin Biol Ther* 2022;22(9):1163-1176.

8 Fujinami K, Waheed N, Laich Y, *et al*. Stargardt macular dystrophy and therapeutic approaches. *Br J Ophthalmol* 2024;108(4):495-505.

9 Munis AM. Gene therapy applications of non-human lentiviral vectors. *Viruses* 2020;12(10):1106.

10 Lonfat N, Moreno-Leon L, Punzo C, *et al*. Update on gene therapy clinical trials for eye diseases. *Hum Gene Ther* 2025;36(19-20):1287-1300.

11 Zhang KY, Johnson TV. The internal limiting membrane: Roles in retinal development and implications for emerging ocular therapies. *Exp Eye Res* 2021;206:108545.

12 Xia X, Guo XZ. Adeno-associated virus vectors for retinal gene therapy in basic research and clinical studies. *Front Med (Lausanne)* 2023;10:1310050.

13 Hu ML, Edwards TL, O'Hare F, *et al*. Gene therapy for inherited retinal diseases: progress and possibilities. *Clin Exp Optom* 2021;104(4):444-454.

14 Takahashi VKL, Takiuti JT, Jauregui R, *et al*. Gene therapy in inherited retinal degenerative diseases, a review. *Ophthalmic Genet* 2018;39(5):560-568.

15 Leclercq B, Mejlachowicz D, Behar-Cohen F. Ocular barriers and their influence on gene therapy products delivery. *Pharmaceutics* 2022;14(5):998.

16 Askou AL, Jakobsen TS, Corydon TJ. Toward lentiviral vectors for antiangiogenic ocular gene therapy. *Mol Ther Meth Clin Dev* 2023;30:443-446.

17 Edelman JL, Castro MR. Quantitative image analysis of laser-induced choroidal neovascularization in rat. *Exp Eye Res* 2000;71(5):523-533.

18 Trapani I. Adeno-associated viral vectors as a tool for large gene delivery to the retina. *Genes* 2019;10(4):287.

19 Chien JY, Huang SP. Gene therapy in hereditary retinal dystrophy. *Tzu Chi Med J* 2022;34(4):367-372.

20 Kansara V, Muya L, Wan CR, *et al*. Suprachoroidal delivery of viral and nonviral gene therapy for retinal diseases. *J Ocul Pharmacol Ther* 2020;36(6):384-392.

21 Do JL, Pedroarena-Leal N, Louie M, *et al*. Mechanical disruption of the inner limiting membrane *in vivo* enhances targeting to the inner retina. *Invest Ophthalmol Vis Sci* 2023;64(15):25.

22 Wigg JP, Zhang H, Yang D. A quantitative and standardized method for the evaluation of choroidal neovascularization using MICRON III fluorescein angiograms in rats. *PLoS One* 2015;10(5):e0128418.

23 Si ZB, Zheng YJ, Zhao J. The role of retinal pigment epithelial cells in age-related macular degeneration: phagocytosis and autophagy. *Biomolecules* 2023;13(6):901.

24 Yuan CX, Yuan S, Dedek K. Assessing the barrier function of the retinal pigment epithelium in adult mice using transepithelial electrical resistance measurements and quantitative immunohistochemistry. *Exp Eye Res* 2026;264:110817.

25 Caceres PS, Rodriguez-Boulan E. Retinal pigment epithelium polarity in health and blinding diseases. *Curr Opin Cell Biol* 2020;62:37-45.

26 Campos M, Amaral J, Becerra SP, *et al*. A novel imaging technique for experimental choroidal neovascularization. *Invest Ophthalmol Vis Sci* 2006;47(12):5163-5170.

27 Dalkara D, Kolstad KD, Caporale N, *et al*. Inner limiting membrane barriers to AAV-mediated retinal transduction from the vitreous. *Mol Ther* 2009;17(12):2096-2102.

28 Lee SH, Colosi P, Lee H, *et al*. Laser photocoagulation enhances adeno-associated viral vector transduction of mouse retina. *Hum Gene Ther Meth* 2014;25(1):83-91.

29 Lee SH, Kim YS, Nah SK, *et al*. Transduction patterns of adeno-associated viral vectors in a laser-induced choroidal neovascularization mouse model. *Mol Ther Meth Clin Dev* 2018;9:90-98.

30 Lavinsky D, Cardillo JA, Mandel Y, *et al*. Restoration of retinal morphology and residual scarring after photocoagulation. *Acta Ophthalmol* 2013;91(4):e315-e323.

31 Tackenberg MA, Tucker BA, Swift JS, *et al*. Müller cell activation, proliferation and migration following laser injury. *Mol Vis* 2009;15:1886-1896.

32 Wang C, Zhang RR, Zhang Q, *et al*. Cytokine profiles and the effect of intravitreal aflibercept treatment on experimental choroidal neovascularization. *Ophthalmic Res* 2022;65(1):68-76.

33 Tu YY, Luo YL, Zhao QL, *et al*. Role of macrophage in ocular neovascularization. *Heliyon* 2024;10(10):e30840.

34 Trapani I, Banfi S, Simonelli F, *et al*. Gene therapy of inherited retinal degenerations: prospects and challenges. *Hum Gene Ther* 2015;26(4):193-200.